Published OnlineFirst November 13, 2012; DOI: 10.1158/0008-5472.CAN-12-1321

Bcl3 Selectively Promotes Metastasis of ERBB2-Driven Mammary Tumors

Alison Wakefield[1], Jitka Soukupova[1], Amelie Montagne[1], Jill Ranger[2], Rhiannon French[1], William J. Muller[2], and Richard W. E. Clarkson[1]

Abstract

Bcl3 is a putative proto-oncogene deregulated in hematopoietic and solid tumors. Studies in cell lines suggest that its oncogenic effects are mediated through the induction of proliferation and inhibition of cell death, yet its role in endogenous solid tumors has not been established. Here, we address the oncogenic effect of Bcl3 *in vivo* and describe how this Stat3-responsive oncogene promotes metastasis of ErbB2-positive mammary tumors without affecting primary tumor growth or normal mammary function. Deletion of the *Bcl3* gene in ErbB2-positive (MMTV-Neu) mice resulted in a 75% reduction in metastatic tumor burden in the lungs with a 3.6-fold decrease in cell turnover index in these secondary lesions with no significant effect on primary mammary tumor growth, cyclin D1 levels, or caspase-3 activity. Direct inhibition of Bcl3 by siRNA in a transplantation model of an Erbb2-positive mammary tumor cell line confirmed the effect of Bcl3 in malignancy, suggesting that the effect of Bcl3 was intrinsic to the tumor cells. Bcl3 knockdown resulted in a 61% decrease in tumor cell motility and a concomitant increase in the cell migration inhibitors Nme1, Nme2, and Nme3, the GDP dissociation inhibitor Arhgdib, and the metalloprotease inhibitors Timp1 and Timp2. Independent knockdown of Nme1, Nme2, and Arhgdib partially rescued the Bcl3 motility phenotype. These results indicate for the first time a cell-autonomous disease-modifying role for Bcl3 *in vivo*, affecting metastatic disease progression rather than primary tumor growth. *Cancer Res; 73(2); 745–55. ©2012 AACR.*

Introduction

HER2-overexpressing tumors are a clinically aggressive subtype of breast cancer resulting in poor prognosis and increased incidence of metastases. Current therapy for HER2-positive breast cancer involves the use of receptor targeted drugs such as the humanized monoclonal antibody, trastuzumab (Herceptin), which, in combination with chemotherapy, can delay disease progression in patients with metastatic disease (1, 2). However, because of prevalent *de novo* and acquired resistance mechanisms, relapse is common. Therefore, there is a need to identify new or synergistic therapeutic molecular targets for HER2-positive breast cancer and to identify mechanisms to suppress disease progression in this poor prognosis patient group.

A recent study of primary human breast tumor cells identified an interleukin (IL)-6/Stat3 autocrine loop in HER2-overexpressing breast cancers that enhanced the aggressive HER2 tumor phenotype *in vivo* (3). Furthermore, Stat3 has been shown to promote malignancy through the transcriptional regulation of inflammatory mediators in a mouse model of HER2-positive disease (mmtv-Neu; ref. 4). Previously, we had identified a panel of genes from murine mammary epithelial cells that were responsive to Stat3 (5). One of these Stat3-responsive genes, *Bcl3*, is a proto-oncogene originally described in B-cell lymphomas that has previously been shown to be constitutively expressed in a small study of breast cancer tissues (6, 7). The precise role for Bcl3 in tumor pathology is currently unknown, but studies in cell lines suggest that it upregulates cell proliferation and survival (8–12). Similarly, there is no known role for Bcl3 in either the normal or neoplastic mammary gland, yet is a cofactor of the inflammatory mediator NF-κB (6), which is associated with mammary epithelial cell survival (13) and malignant progression in HER2- and EGFR1-positive mammary tumors (14–16). We have previously proposed that Bcl3 may act as a link between Stat3 and NF-κB signaling *in vivo* (5, 17).

Here, we have used mouse models of HER2-positive breast cancer to determine for the first time the direct oncogenic effect of Bcl3 *in vivo*. Stat3-deficient ErbB2 tumors exhibited a reduction in Bcl3 expression, whereas Bcl3 deficiency alone, both in transgenic mice *in vivo* and in xenografts, significantly reduced metastatic tumor burden yet did not affect primary tumor growth. We show that these effects are mediated by Bcl3-dependent regulation of motility/invasion-related genes in a tumor cell–autonomous manner. These results highlight a novel disease-modifying role for Bcl3 *in vivo*, which was not

Authors' Affiliations: [1]University of Cardiff School of Biosciences, Museum Avenue, Cardiff, United Kingdom; and [2]Goodman Cancer Centre, McGill University, Montreal, Quebec, Canada

Note: Supplementary data for this article are available at Cancer Research Online (http://cancerres.aacrjournals.org/).

Corresponding Author: Richard W. E. Clarkson, Life Sciences Building, School of Biosciences, University of Cardiff, Museum Avenue, Cardiff, Wales CF10 3AX, United Kingdom. Phone: 02920-870249; Fax: 02920-876328; E-mail: clarksonr@cf.ac.uk

doi: 10.1158/0008-5472.CAN-12-1321

Published OnlineFirst November 13, 2012; DOI: 10.1158/0008-5472.CAN-12-1321

predicted from earlier *in vitro* studies. In the light of these results and the current limitations in targeting Stat3 and NF-κB pathways directly, we discuss the potential for Bcl3 as a new alternative therapeutic target for HER2-positive breast cancer.

Materials and Methods

Mouse models and tissue harvests

All animal experiments were carried out in accordance with UK Government Home Office guidelines. The generation of mice with a mammary-specific deletion of Stat3 in normal (*Blg-Cre/Stat3*$^{fl/-}$) and neoplastic mammary tissues (Stat3/N_2: Stat3$^{fl/fl}$/(NIC)mmtv-N2/mmtv-Cre) have been described previously (4, 18). Bcl3/N_2 mice were generated from mmtv-N_2 (19) and Bcl3$^{-/-}$ (20) lines. Animals were inspected for mammary tumors by palpation, and tumors were measured twice weekly with calipers. Animals were euthanized when tumors reached 2 cm and tissues either snap frozen in liquid nitrogen for protein or RNA analysis or fixed in formalin for histology. For pregnancy cycle and involution studies, mammary tissue from fourth abdominal glands was collected at the indicated time points and formalin fixed for histology. For whole mounts, fourth abdominal glands were incubated in Carnoy solution for 2 to 4 hours and then stained in Carmine solution overnight. For secondary tumor studies, 1:30 serial sections were assessed for the entire depth of the tissue and stained for histology.

Cell culture

The MG1361 murine mammary tumor cell line (21) and the EPH4 normal murine mammary epithelial cell line were obtained from Prof. C. Watson (Department of Pathology, Cambridge University, Cambridge, UK). The N202A and N202E murine mammary tumor cell lines were gifts from Prof. P.-L. Lollini (Sezione di Cancerologia) and the 4T1 murine mammary tumor cell line was a gift from Dr. R. Anderson (Department of Pathology, University of Melbourne, Melbourne, VIC, Australia). The human breast cancer cell lines, MDA-MB-231 and SKBR3, were a gift from Dr. Julia Gee (Department of Pharmacy, Cardiff University, Cardiff, UK). The HCC1954 human breast cancer cell line was a gift from Dr. Mohamed Bentires-Alj (Friedrich Miescher Institute for Biomedical Research, Basle, Switzerland) and the ZR-75-1 human breast cancer cell line was a gift from Prof. Wen Jiang (Wales College of Medicine, Cardiff University). Eph4 and human lines cells were maintained in Dulbecco's modified Eagle's medium (DMEM) supplemented with 10% v/v FBS (Sigma), penicillin (50 units/mL; Invitrogen), streptomycin (50 units/mL; Invitrogen), and L-glutamine (2 mmol/L; Invitrogen). The N202A and N202E cell lines were maintained in the same media as above but supplemented with 15% v/v FBS. The MG1361 cell line was maintained in Williams Media E (Invitrogen) supplemented with L-glutamine (2 mmol/L), penicillin (50 units/mL), streptomycin (50 μg/mL), 15% v/v FBS, and 5 mL nonessential amino acids (Sigma). The 4T1 cell line was maintained in RPMI (Invitrogen) supplemented with 10% v/v FBS, penicillin (50 units/mL; Invitrogen), streptomycin (50 units/mL; Invitrogen), and L-glutamine (2 mmol/L; Invitrogen). All cell lines were incubated at 37°C and 5% CO_2. Cells were reverse-transfected with ON-TARGET plus SMARTpool siRNA (Dharmacon) targeting the genes indicated and an irrelevant control RNA, using Lipofectamine RNAiMAX (Invitrogen) according to the manufacturer's protocols.

Quantitative RT-PCR

RNA was isolated from frozen tissues and cells by RNeasy (Qiagen) and cDNA obtained using Revertaid (Fermentas) reverse transcriptase and random primers (Promega) according to manufacturer's instructions. Quantitative PCR was carried out using SyBr green as previously described (22). Primers, available on request, were generated against the following mouse sequences: Nme1 (NM_008704.2); Nme2 (NM_008705.4); Nme3 (NM_019730.1); Timp1 (NM_011593.2); Timp2 (NM_011594.3); Arhgdib (NM_007486.1); Bcl3 (NM_033601.3); Cyclin D1 (NM_007631.2); and the human sequence Bcl3 (NM_005178.4).

Western blotting

Frozen mammary tumor tissues and cell pellets were lysed using radioimmunoprecipitation assay (RIPA; ref. 22) buffer and run on SDS-PAGE gels. Proteins were detected using antibodies directed against Neu (1:200, Abcam, Cat# Ab2428), EGFR (1:1000, Cell Signalling Technologies, Cat# 2232), Vimentin (1:200, Santa Cruz, Cat# SC-7557), E-cadherin (1:500, Upstate, Cat# 07-697), Snail (1:500, Santa Cruz. Cat# Sc-10433), and Tubulin (1:10000, Abcam, Cat# Ab6160).

Microarray analysis

RNA was extracted and treated with Deoxyribonuclease I Amplification Grade (Invitrogen) to remove any contaminating gDNA. Microarray analysis was conducted using an Illumina MouseRef-8 version 2 BeadChip. Comparisons between data sets were conducted by the using the R-package Limma (23). Samples were ranked according to adjusted *P* values obtained from *t* tests corrected for multiple testing.

Immunohistochemistry

Mammary glands or tumors were fixed in 4% paraformaldehyde before paraffin embedding and sectioning. Ten-micrometer sections were incubated in 1:20 anti-Ki67 (Vector Labs, Mouse monoclonal, VP-K452) in 20% normal rabbit serum in PBST, 1:200 anti-cleaved caspase-3 (Asp 175, Cell Signalling, Rabbit polyclonal, 9661) in PBST, or 1:100 anti-Bcl3 (H-146, Santa Cruz, sc-13038) in 20% normal goat serum in PBS, with prior avidin/biotin block (Vector Laboratories) at 4°C overnight. Primary antibody was incubated with biotinylated secondary antibodies [rabbit anti-mouse (Dako) 1:200 in 20% normal rabbit or goat serum in PBS(T) for Ki67 and Bcl3 respectively or goat anti-rabbit (Dako) 1:200 in 5% bovine serum albumin (Sigma) in PBST for cleaved caspase-3] and detected using ABC complex (Vector Laboratories) and DAB chromogen (Vector Laboratories). Nuclei were counterstained with hematoxylin before mounting.

Boyden chamber migration assay

Migration assays were conducted using modified Boyden chambers with filter inserts for 24-well dishes containing 8-μm

Published OnlineFirst November 13, 2012; DOI: 10.1158/0008-5472.CAN-12-1321

pores (Becton Dickinson). Forty-eight hours after transfection, 70,000 cells were plated into 400 μL of media supplemented with 0.2% serum in the upper chamber, and the lower chamber was filled with 750 μL of media supplemented with 10% serum. After 24 hours in culture, cells were fixed in 70% ice-cold ethanol overnight before staining with Harris hematoxylin and eosin (H&E). Filters were mounted on glass slides and counted by microscopic inspection. The same procedure was used for invasion assays apart from BD BioCoat Growth Factor Reduced Matrigel Invasion chambers were used and cells were incubated for 48 hours. For each experiment, cells were counted in 2 fields of view from 2 membranes for each condition.

Fluorescence-activated cell sorting

Transfected cells were washed in PBS/2% FBS, resuspended in 100 μL of fluorescein isothiocyanate (FITC)-conjugated anti-CD24 (BD Pharmingen) or phycoerythrin (PE)-conjugated anti-Sca1 (BD Pharmingen) and left on ice for 30 minutes in the dark. Cells were washed twice in PBS/2% FBS before fluorescence-activated cell sorting (FACS) using a FACSAria Flow Cytometer (BD Biosciences) and analysis conducted with FlowJo software. Gates were set to exclude more than 99% of cells labeled with isoform-matched control antibodies conjugated with the corresponding fluorochromes.

Aldefluor reagents (Stemcell Technologies) were prepared according to manufacturer's instructions. Transfected cells were suspended at 1×10^6 cells/mL with 5 μL of activated Aldefluor substrate per mL. All samples were incubated for 45 minutes (±DEAB) at 37°C. FACS was conducted as above with gates set to exclude more than 99% of control cells incubated with DEAB.

Mammospheres assay

Cells were resuspended in mammosphere culture medium [serum-free epithelial growth medium (MEBM, Lonza), supplemented with B27 (Invitrogen), 20 ng/mL EGF (Sigma), 5 mg/mL insulin (Sigma), 0.0008% v/v β-mercaptoethanol (Sigma), and 1 mg/mL hydrocortisone (Sigma)], counted and seeded into ultra-low attachment plates (Corning) at a density of 4,000 cells/mL and incubated for 7 days at 37°C and 5% CO_2, after which mammospheres were counted. To determine the self-renewal capacity of cells, mammospheres were collected by gentle centrifugation at 1,100 rpm and dissociated into single cells before being reseeded into ultra-low attachment plates at a density of 4,000 cells/mL. Cells were then incubated for 7 days at 37°C and 5% CO_2 before counting.

Experimental metastases models

MG1361 cells were transfected with Bcl3 or control siRNA for 48 hours and harvested using Tryspin/EDTA, washed, and disaggregated into single-cell suspensions before being resuspended at 4×10^6 cells/mL in serum free L-15 media (Invitrogen), 200 μL of cell suspension was injected into the lateral tail vein of 6- to 8-week-old female virgin BALBc/SCID mice. Animals were left for 21 days before being culled by cervical dislocation. Lungs were dissected photographed and fixed in 4% formalin before being processed for H&E staining.

Statistical analyses

The Mann–Whitney *U* test was used to determine statistical differences between nonparametric data sets. The Student *t* test was used to determine statistical differences between normally distributed data sets and between data sets with sample sizes of $n = 3$. The χ^2 test was used to determine statistical differences between observed frequencies and expected frequencies of data.

Results

Bcl3 is elevated in ErbB2-positive mammary tumor cells but does not affect tumor growth

We have previously reported that expression of the NF-κB cofactor Bcl3 is dependent on Stat3 in mammary epithelial cells (5). This was confirmed for both Bcl3 mRNA and protein levels in normal mammary tissues (Fig. 1A) and in ErbB2-positive mammary tumors (Fig. 1B). Bcl3 protein was predominantly expressed in the majority of nuclei of tumor cells, whereas in normal mammary epithelium, Bcl3 was preferentially localized within the cytoplasm of luminal epithelial cells and a minority of epithelial nuclei. Bcl3 expression was also observed to be constitutively elevated in ErbB2-positive mouse mammary (Fig. 1C) and human breast tumor cell lines (Supplementary Fig. S1). We wished to determine, therefore, whether Bcl3 contributed directly to the progression of ErbB2 mammary tumors *in vivo* and furthermore whether this correlated with the tumorigenic effects of Stat3 previously observed in this tumor subtype.

Bcl3-deficient mice (20) were crossed with the mmtv-ErbB2/neu (N_2) transgenic mouse line, a model of metastatic breast cancer (19). $Bcl3^{-/-}N_2$ mice developed focal primary mammary adenocarcinomas that were comparable with those formed in wild-type N_2 mice both in terms of their growth rate (Fig. 2A) and in histologic appearance (Supplementary Fig. S2). This was confirmed at the cellular level where molecular markers of apoptosis, mitosis, and ErbB/ErbB2 expression were unchanged in $Bcl3^{-/-}N_2$ tumors compared with wild-type N_2 controls (Fig. 2B and C; Supplementary Fig. S2). Furthermore, the cell-cycle regulator cyclin D1, a known NF-κB/Bcl3–responsive gene (11), was not significantly altered by the absence of Bcl3 expression (Fig. 2D).

Similar results were also observed during early tumorigenesis whereby the incidence, histology, and cell turnover kinetics of preneoplastic mammary epithelial hyperplasias were unaffected by Bcl3 loss (Supplementary Fig. S3).

Thus, unlike previous reports on the effects of Stat3 (4) and components of the IKK/NF-κB pathway (24, 25) in ErbB2 tumors, loss of Bcl3 did not affect mammary tumor growth *in vivo*.

Bcl3 deficiency reduced the occurrence of lung metastases in ErbB2 transgenic mice

In addition to the potentiation of tumor growth, Stat3 was previously shown to promote malignancy in ErbB2-positive tumors (4). The role of NF-κB in the metastatic progression of ErbB2 tumors *in vivo* has not been previously reported, yet there is a body of evidence, in breast cancer cell lines *in vitro*, to

Published OnlineFirst November 13, 2012; DOI: 10.1158/0008-5472.CAN-12-1321

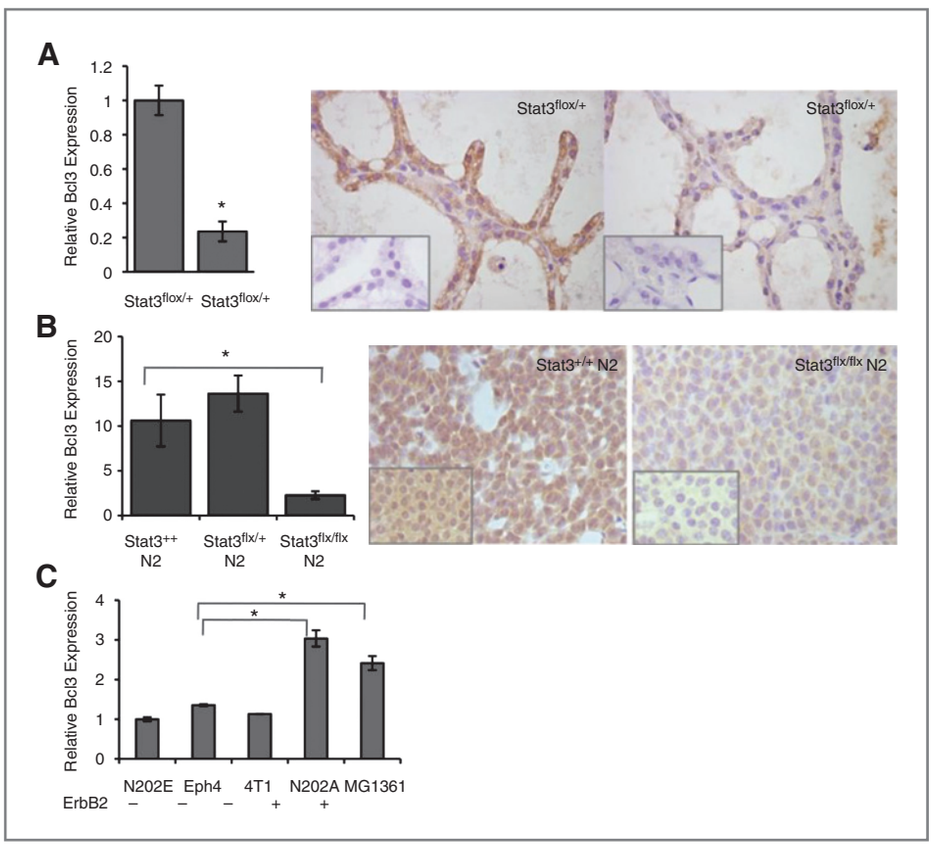

Figure 1. Bcl3 is potentiated by Stat3 and ErbB2. *Bcl3* expression as measured by quantitative RT-PCR (qRT-PCR) relative to cyclophilin B (histograms) and immunohistochemistry (images) in Blg/Cre/Stat3$^{flox/+}$ and Blg/Cre/Stat3$^{flox/-}$ mammary glands (A) at 18 hour involution (n = minimum of 3). Inset, no primary antibody control. B, Stat3$^{wt/wt}$N$_2$, Stat3$^{flx/wt}$N$_2$, and Stat3$^{flx/flx}$N$_2$ mammary tumors ($n = 10$); *, $P = 0.0108$; t test. Inset, Bcl3 staining in N2 tumors from Bcl3+ (left) and Bcl3- (right) animals. C, mouse mammary tumor cell lines, $n = 3$. Student t Test conducted on all comparisons. *, $P \leq 0.05$.

suggest that NF-κB signaling might contribute directly to malignancy (14–16, 24, 26). N$_2$ mice develop lung metastases with high frequency (19). To determine the influence of Bcl3 in ErbB2 mammary tumor progression, the lungs of Bcl3$^{+/+}$N$_2$ and Bcl3$^{-/-}$N$_2$ mice harboring late-stage primary mammary tumors of the same size (4,000 ± 30 mm^3) were investigated for the presence of secondary tumors by gross examination and histology. As previously described (19), lung metastases with identical cellular morphology to the primary mammary tumor arose with high incidence in N$_2$ mice with large primary lesions (Fig. 3A). Bcl3 deficiency resulted in a 40% reduction in the number of animals with metastatic lesions within the lung (Fig. 3B), and in those remaining animals with metastases, a 75% reduction in tumor burden (Fig. 3C). In contrast to the primary mammary lesions, immunohistochemistry of these secondaries revealed a significant reduction in mitotic index

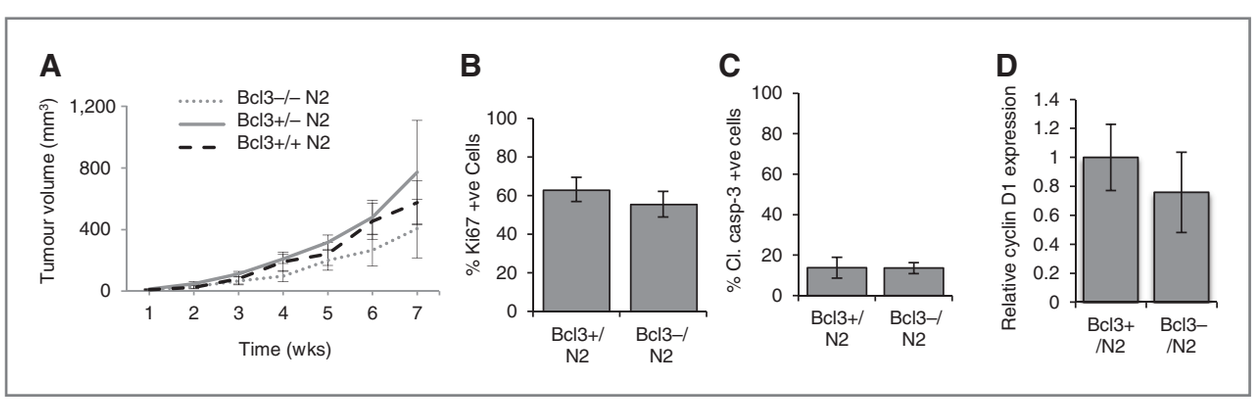

Figure 2. ErbB2 tumor growth is unaffected by Bcl3 loss. A, growth rates of Bcl3$^{+/+}$N$_2$, Bcl3$^{+/-}$N$_2$, and Bcl3$^{-/-}$N$_2$ primary mammary tumors (n = minimum of 16). Mann–Whitney U test within time points determined no significant differences at $P = 0.05$. B, percentage of Ki-67–positive and (C) cc3-positive cells in Bcl3$^{+/+}$N$_2$ and Bcl3$^{-/-}$N$_2$ tumors by immunohistochemistry (see Supplementary Fig. S1C). D, qRT-PCR of cyclin D1 relative to cyclophilin B in Bcl3$^{+/+}$N$_2$ and Bcl3$^{-/-}$N$_2$ mammary tumors. Error bars, SEM. Student t test conducted on all comparisons (B–D) exhibited no significant differences at $P = 0.05$.

Published OnlineFirst November 13, 2012; DOI: 10.1158/0008-5472.CAN-12-1321

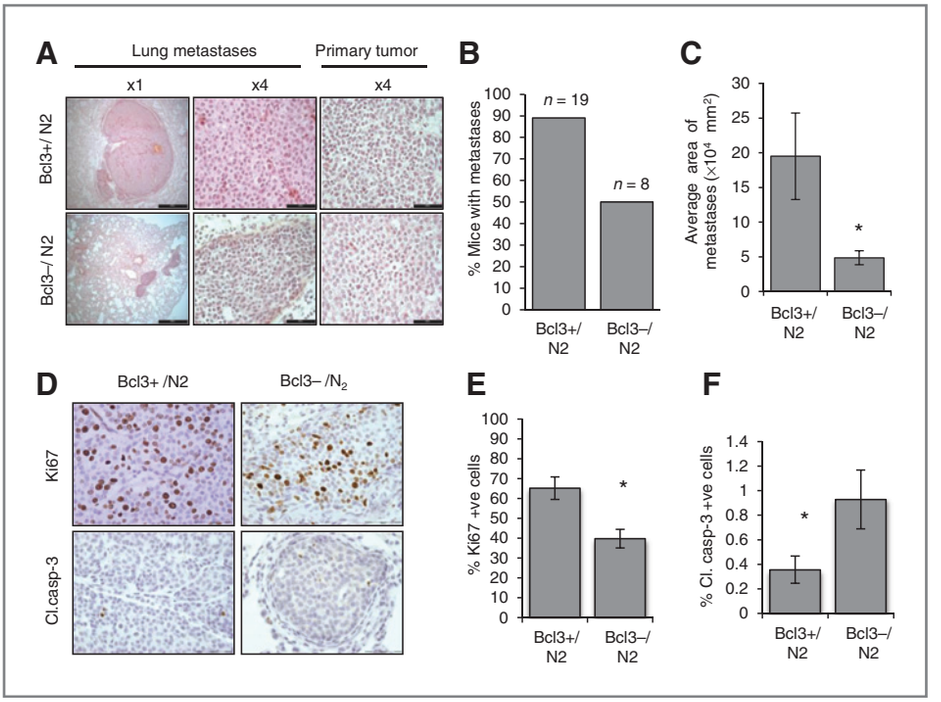

Figure 3. Bcl3 deficiency reduces ErbB2 metastatic tumor burden. A, histology of $Bcl3^{+/+}N_2$ and $Bcl3^{-/-}N_2$ lung metastases and primary tumors. Scale bars, left, 500 μm; right and middle, 50 μm. B, percentage of mice harboring metastatic lesions in the lung. C, average area of secondary lesions in animals presenting with lung metastases. *, Mann–Whitney *U* test. $P \leq 0.01$. D, Ki-67 and cc3 immunohistochemical staining of $Bcl3^{+/+}N_2$ and $Bcl3^{-/-}N_2$ metastatic lung lesions. Scale bars, 50 μm. Quantification of the percentage of Ki-67 (E)- or cc3-positive (F) cells from 3 sections per lesion, $n = 6$. *, Mann–Whitney *U* test. $P \leq 0.05$. Error bars, SEM.

(Ki-67) and a modest increase in apoptosis (cleaved caspase-3; cc3), resulting in a 3.6-fold decrease in cell turnover index (CTI; ref.27) in $Bcl3^{-/-}N_2$ metastases (38% Ki-67 vs. 0.93% cc3) compared with $Bcl3^{+/+}N_2$ controls (52% Ki-67 vs. 0.36% cc3; Fig. 3D–F).

Thus, deletion of Bcl3 exerted dual effects on ErbB2 tumor cells resulting in a dramatic reduction in metastatic tumor burden: a decrease in secondary tumor colonization (unrelated to primary tumor size or growth) and a reduction in metastatic tumor growth—a property not seen at the primary site.

Bcl3 deficiency had no effect on normal epithelial morphogenesis and remodeling

NF-κB and Stat3 are differentially regulated during the course of adult mammary gland development and play key roles in epithelial homeostasis within the mammary gland (18, 28–30). Targeted inhibition of components of these signaling pathways is therefore detrimental to normal mammary (and other tissue) function and as such diminishes their use for therapeutic intervention in breast cancer, despite their well-characterized role in tumorigenesis.

Bcl3 exhibits a distinct expression pattern in the mouse mammary gland during the adult pregnancy cycle (Fig. 4A; refs. 5, 13) compared with its cognate NF-κB–binding partners p50 (Nfkb1) and p52 (Nfkb2). To determine whether Bcl3 affected the mammary epithelial compartment *in vivo*, we compared mammary ductal morphology and epithelial architecture between $Bcl3^{-/-}$ mice and their littermate controls during pubertal development and in the adult pregnancy cycle (Fig. 4B; Supplementary Fig. S4). $Bcl3^{-/-}$ mice exhibited no differences in epithelial architecture or tissue homeostasis in the adult mammary gland. Luminal epithelial cells exhibited the characteristic morphologic appearance of secretory cells during lactation and litters were reared successfully with no signs of reduced vitality, indicating that epithelial function was also unaffected. Epithelial regression and remodeling during postlactational involution was also undisturbed, despite the transient increase in Bcl3 at the onset of involution in wild-type Bcl3 animals (Fig. 4C and D).

Global suppression of Bcl3 therefore had no effect on normal mammary epithelial homeostasis, highlighting a tumor-specific role for Bcl3 in ErbB2-overexpressing cancers.

The reduction in metastases was due to a tumor cell–autonomous effect independent of stem/progenitor numbers

The substantial decrease in metastasis incidence in $Bcl3^{-/-}$ N2 animals suggested that Bcl3 promoted the dissemination and/or colonization of tumor cells to distal sites, a complex process that involves interaction between tumor cells and the neighboring stromal environment. This raised the question of whether Bcl3 mediated its effects directly within the tumor cells or whether the absence of Bcl3 in the surrounding tissues of the Bcl3-null mice indirectly mediated the reduction in tumor metastasis.

To address this, Bcl3 was inhibited in an ErbB2-positive mammary tumor cell line derived from an activated Neu/ErbB2 mammary tumor (MG1361; ref. 21) and transplanted into recipient animals with normal levels of Bcl3. Introduction of Bcl3-deficient cells into the bloodstream of recipient mice, resulted in an 80% reduction in metastases to the lung compared with control xenografts, consistent with the phenotype observed in transgenic animals (Fig. 5A and B). Thus, Bcl3

Published OnlineFirst November 13, 2012; DOI: 10.1158/0008-5472.CAN-12-1321

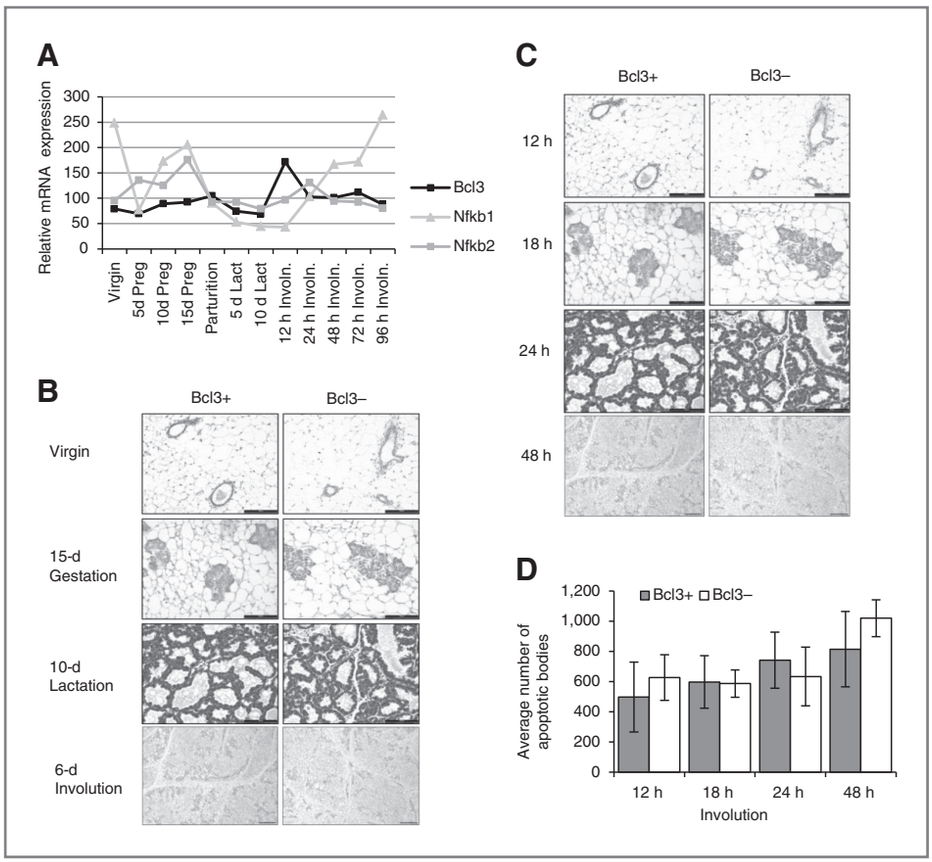

Figure 4. Bcl3 deficiency has no effect on normal mammary epithelial architecture. A, *Bcl3*, *NF-κB1*, and *NF-κB2* expression during the mouse mammary pregnancy cycle as determined by microarray analysis (55). B, representative histology of $Bcl3^{+/+}$ and $Bcl3^{-/-}$ mouse mammary glands at virgin, 15-day gestation, 10-day lactation, and 6-day involution time points, $n = 3$. Scale bars, 100 μm. C, histology of $Bcl3^{+/+}$ and $Bcl3^{-/-}$ mouse mammary glands at 12, 18, 24, and 48 hours of involution, $n = 4$. Scale bar, 200 μm. D, number of shed apoptotic bodies per field of view (3 per section) at each involution time point. $n \geq 4$ mice. Student *t* test revealed no significant differences.

mediated its prometastatic effect intrinsically within the tumor cells. The transient nature of Bcl3 inhibition in this model however meant that it was not possible to assess the effect of Bcl3 on cell growth *in vivo*. Consequently, we assessed the role of Bcl3 on cell turnover *in vitro* (Fig. 5C). No differences either in cell number or viability were observed following suppression of Bcl3 in adherent monolayer culture, suggesting that the effect on metastatic tumor growth and CTI observed *in vivo* may be mediated indirectly by the tumor microenvironment within the lung.

Tumor incidence and metastatic properties of HER2/ErbB2-positive tumors have previously been ascribed to the expansion of a tumor-initiating (stem/progenitor) cell subpopulation, mediated by HER2 signaling. Furthermore canonical NF-κB signaling has been shown to influence the size of the stem/progenitor population in a 7,12-dimethylbenz(*a*)anthracene (DMBA) mammary tumor model in mice (31). The stem/progenitor markers Sca1 and CD24 have independently been shown to enrich for tumor-initiating cells in mmtv-Neu and mmtv-NeuT tumor cell populations respectively (32, 33). We used a combination of functional stem/progenitor assays and surrogate markers in flow cytometry to assess whether the effect of Bcl3 inhibition on metastasis of MG1361 cells correlated with changes in stem/progenitor subpopulations. We found no changes in stem/progenitor numbers to explain the reduction in secondary tumor seeding observed in Bcl3-deficient tumor cells (Supplementary Fig. S5).

Bcl3-deficient tumor cells exhibited reduced motility

To identify the underlying mechanism responsible for the cell-autonomous effect of Bcl3 on secondary tumor burden, several key cellular properties associated with metastasis were assessed in Bcl3-deficient tumor cells.

Prometastatic tumor cells disseminated in the blood stream must overcome proapoptotic stresses imparted by cell detachment to seed distal sites. We therefore determined the sensitivity of MG1361 cells to cell detachment *in vitro*. No differences in cell viability were observed between Bcl3-deficient and wild-type tumor cells (Fig. 6A), suggesting that Bcl3 did not affect the ability of detached cells to undergo anoikis.

Metastasis is also associated with epithelial-to-mesenchymal transition (EMT) of tumor cells, a genetically programmed event that encompasses changes in cell shape, motility, and adhesion. Boyden chamber assays determined that Bcl3 promoted cell motility of ErbB2-positive cells. Bcl3 suppression resulted in a 61% reduction in the migratory capacity of MG1361 cells (Fig. 6B), with those cells that had migrated expressing normal levels of Bcl3 mRNA (Supplementary Fig. S6). Furthermore, global gene expression analysis revealed that a number of motility-associated genes were differentially expressed following siRNA-mediated suppression of Bcl3 in MG1361 cells (Table 1), including 4 members of the Nme (NM23) family of nucleoside diphosphate kinase/transcription co-activator genes, of which Nme1, in particular has been shown to be involved in the inhibition of cell motility and

Published OnlineFirst November 13, 2012; DOI: 10.1158/0008-5472.CAN-12-1321

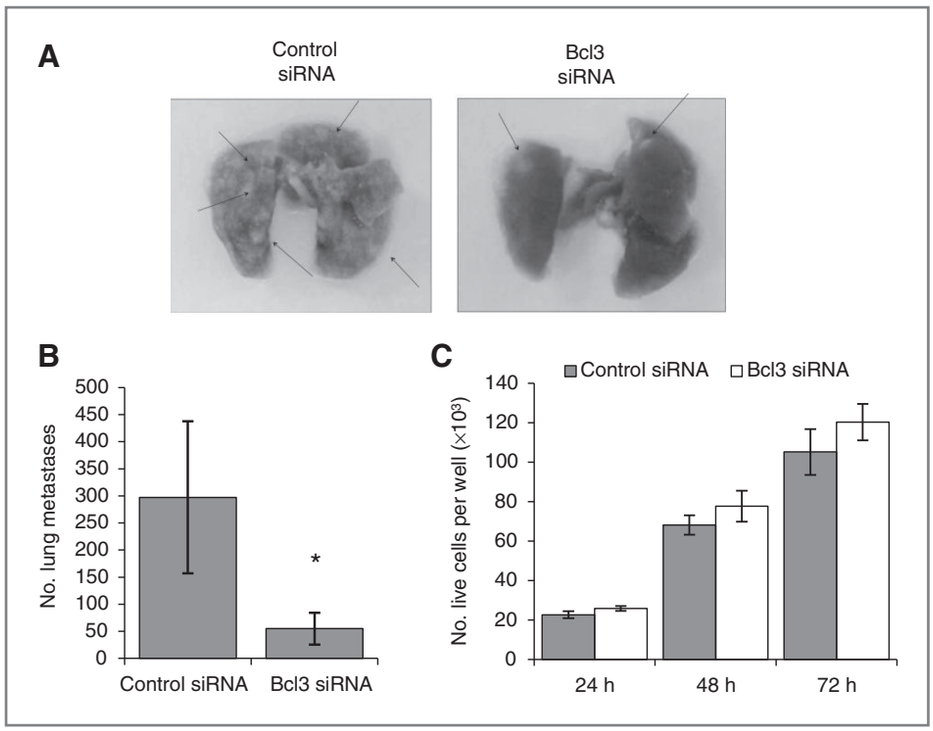

Figure 5. Bcl3-deficient ErbB2 xenografts exhibit reduced metastatic tumor burden. A, representative images of excised lungs from immunodeficient mice ($n = 5$) that had received xenografts of Bcl3 siRNA or control MG1361 cells. B, quantification of number of lung metastases per mouse identified by serial section of whole lungs. *, Mann–Whitney *U* test, $P \leq 0.05$. C, number of trypan blue–negative MG1361 cells in adherent cell culture following 48-hour transfection with Bcl3 or control siRNA. Error bars, SEM. Student *t* test revealed no significant differences.

metastases in various model systems including breast cancer (34–36). Quantitative PCR was used to confirm the differential expression of these genes (Fig. 6C). Similarly, the Rho GDP dissociation inhibitor, Arhgdib, was confirmed to be upregulated following Bcl3 suppression (Fig. 6C). This inhibitor of GDP–GTP exchange has previously been implicated in the dynamic regulation of skeletal filaments within tumor cells that controls cell motility (37, 38) and is associated with malignant progression in breast cancer (39). To confirm the relevance of these transcriptional changes, we investigated the motility of ErbB2-positive mammary tumor cells following suppression of Nme 1, 2, and 3 and Arhgdib and also observed their effect on Bcl3-dependent motility (Fig. 6D). Thus, RNA interference (RNAi)-mediated suppression of Arhgdib, Nme1, and Nme2 increased motility of MG1361 cells as expected. No significant effect was observed with Nme3. Furthermore, knockdown of Arhgdib, Nme1, and Nme2 gene expression each partially restored the loss of motility observed with Bcl3 RNAi, suggesting that the negative regulation of both Nme and Arhgdib contributed to the observed mobilization of tumor cells by Bcl3 (Fig. 6D).

Analysis of the EMT markers E-cadherin, N-cadherin, and their upstream transcriptional regulator Snail failed to identify significant changes in gene expression following Bcl3 RNAi, suggesting that Bcl3 specifically influenced cell motility but did not regulate cell adhesion associated with EMT (Supplementary Fig. S7).

An additional property of metastatic cells is the ability to invade tissues through the local production of proteases either directly from the tumor itself or in a juxtacrine manner through cross-talk with the adjacent microenvironment. We assessed the invasive property of Bcl3-depleted MG1361 cells in Matrigel-coated Transwells and observed a significant decrease in the ability of Bcl3-deficient cells to migrate through the matrix (Fig. 6E). However, as the relative decrease in invasive cells was equivalent to the reduction in cell motility, it is likely that the motility phenotype was primarily responsible for the observed effect in the invasion assay. Despite this, microarray data verified by quantitative PCR identified a Bcl3-dependent decrease in Tissue Inhibitor of Metalloprotease 1 and 2 (Timp1, Timp2), key inhibitors of tumor-associated MMPs (Fig. 6C) (40). Taken together these data indicate that Bcl3 plays a tumor-specific role in promoting cell migration/invasion of ErbB2-positive mammary tumors.

Discussion

As its original identification at the locus of a chromosomal breakpoint in chronic lymphocytic leukemia, Bcl3 has been shown to be aberrantly expressed in several solid tumor types, including breast, endometrial, colorectal, and nasopharangeal carcinomas (7, 41–43). Despite this, the role of Bcl3 in endogenous tumor pathology is poorly defined. Previous studies have focused on the effects of Bcl3 in tumor cell lines and have identified roles in proliferation (8–11) and cell survival (12) *in vitro*, whereas one study showed that ectopic expression of Bcl3 in an estrogen receptor (ER)-positive breast cancer cell line (MCF-7) promoted hormone-independent growth in xenografts (44). Here, we addressed the role of Bcl3 in endogenous tumor development *in vivo*, using a transgenic mouse model of spontaneous breast cancer progression. We describe a distinct disease-modifying role for Bcl3 in ErbB2-positive mammary tumors in which Bcl3 has no significant role in growth of the

Published OnlineFirst November 13, 2012; DOI: 10.1158/0008-5472.CAN-12-1321

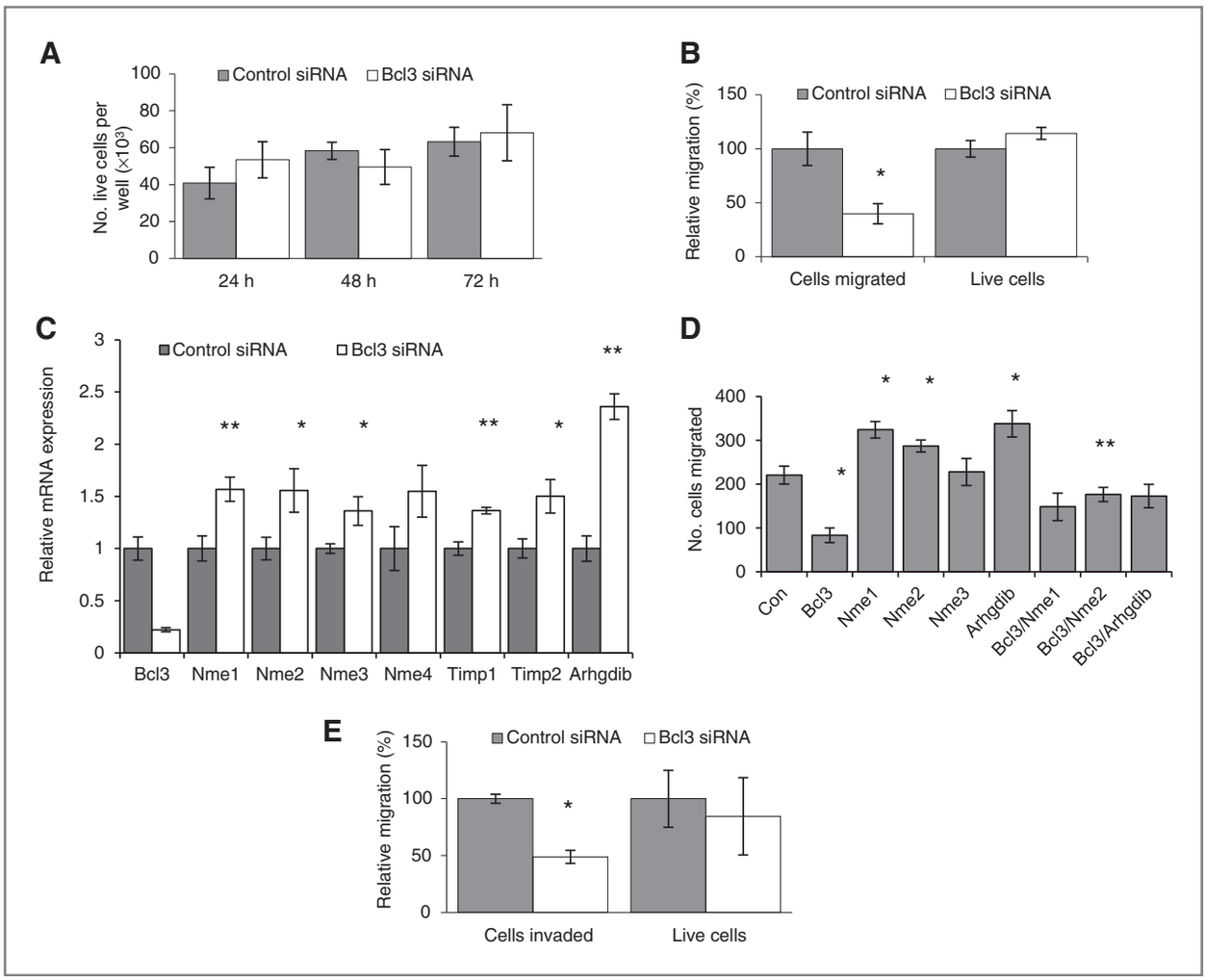

Figure 6. Bcl3-induced cell migration is mediated by suppression of motility genes. MG1361 cells were transfected for 48 hours with Bcl3 or control siRNA before assessment of the number of trypan blue–negative cells in nonadherent cell culture (A); the number of migrated cells in a 24-hour Boyden chamber assay (left) or the number of live cells remaining after 24 hours in adherent growth conditions (right; B), Mann–Whitney *U* test. *, $P \leq 0.05$. C, *Bcl3*, *Nme1-4*, *Arhgdib*, and *Timp1-2* mRNA expression in Bcl3 and control siRNA–transfected MG1361 cell lines as measured by qRT-PCR relative to *cyclophilin B*. *, *t* test, $P \leq 0.05$; **, *t* test, $P \leq 0.01$. D, migration of MG1361 cells following siRNA-mediated knockdown of Nme1, Nme2, Nme3, or Arhgdib alone or in combination with Bcl3 siRNA, normalized to the untreated (scrambled RNAi) control. *, paired *t* test $P < 0.05$ versus control; **, paired *t* test $P < 0.05$ versus Bcl3. E, migration of MG1361 cells in Matrigel-coated Boyden chambers following siRNA-mediated knockdown of Bcl3, normalized to the untreated (scrambled RNAi) control. *T* test was conducted on invaded cells and live cells. *, $P \leq 0.05$. All data represent the mean of 3 independent experiments.

primary tumor but profoundly affects the intrinsic ability of mammary tumor cells to colonize at distal sites. This correlated with an increase in cell migration, mediated by Bcl3-dependent regulation of several motility-associated genes, each of which contributed to the motility phenotype.

Bcl3, which mediates gene transcription through interaction with the NF-κB subunits p50 and p52, appears to alter a distinct subset of malignancy-associated genes from its NF-κB dimeric partners (14, 16). Thus, global suppression of NF-κB signaling in mammary epithelial cells had previously been found to impact on the metastasis-associated genes *CXCR4*, *VEGF1*, and *MMP9*, distinct from the motility inhibitors Nme1, Nme2, and Arhgdib identified here to be responsive to Bcl3. There is much interest in the use of NF-κB inhibitors to suppress tumor progression in cancer, but global inhibition of NF-κB signaling has a profound effect on homeostasis of normal tissues, particularly on cells of the immune system (45). In the mammary gland, tissue-specific inhibition of NF-κB activity has deleterious effects on lobuloalveolar remodeling during pregnancy (30) and post-lactational involution (28). Therapeutic targeting of NF-κB in disease is therefore likely to have severe consequences on normal tissues. An alternative strategy of NF-κB targeted therapy has therefore been proposed, which involves a more selective inhibition of NF-κB signaling through the putative targeting of cofactors or upstream regulators of NF-κB (45–47). Thus, the selective regulation of malignancy-associated gene targets by Bcl3 and the fact that mice with constitutive Bcl3 deficiency are viable with only minor immunologic defects (20, 48), and no detrimental effects on normal mammary gland morphology or

Published OnlineFirst November 13, 2012; DOI: 10.1158/0008-5472.CAN-12-1321

Table 1. Bcl3-regulated genes were determined by microarray analysis of MG1361 cells transfected with Bcl3 or control siRNA for 48 hours

Accession number	Definition	*P*
NM_008704.2	Nonmetastatic cells 1 (NM23A; (Nme1)	0.00092
NM_008705.4	Nonmetastatic cells 2 (NM23B; Nme2)	0.00062
NM_019730.1	Nonmetastatic cells 3 (Nme3)	0.00332
NM_019731.1	Nonmetastatic cells 4 (Nme4)	0.000006
NM_011593.2	Tissue inhibitor of metalloproteinase 1 (Timp1)	0.00395
NM_011594.3	Tissue inhibitor of metalloproteinase 2 (Timp2)	0.00633
NM_011595.2	Tissue inhibitor of metalloproteinase 3 (Timp3)	0.00490
NM_007616.3	Caveolin 1 (Cav1)	0.00086
NM_007486.1	Rho, GDP dissociation inhibitor (GDI) beta (Arhgdib)	0.00121
NM_010288.2	Gap junction membrane channel protein alpha 1 (Gja1)	0.00412
NM_010688.2	LIM and SH3 protein 1 (Lasp1)	0.000979
NM_024454.1	Member RAS oncogene family (Rab21)	0.00081
NM_021356.2	Growth factor receptor–bound protein 2-associated protein 1 (Gab1)	0.00980
NM_010513.2	Insulin-like growth factor I receptor (Igf1r)	0.001812
NM_020011.4	Sphingosine kinase 2 (Sphk2)	0.000183
NM_009335.1	Transcription factor AP-2, gamma (Tcfap2c)	0.002948
NM_011577.1	Transforming growth factor, beta 1 (Tgfb1)	0.003077

NOTE: Significantly regulated invasion- and motility-related genes with putative NF-κB binding sites in their proximal promoter regions, as defined by the TRANSFAC database, are listed.

function (Fig. 4) make it a candidate for therapeutic intervention of disease progression in patients with breast cancer.

We found that the majority of Bcl3-responsive genes identified were upregulated following Bcl3 suppression, consistent with a recent study in HeLa cells (49). This supports previous observations that Bcl3 can suppress as well as activate gene transcription (50). A recent study showing enhanced stability of the transcriptional inhibitor CtBP through a protein–protein interaction with Bcl3 (51) provides a possible explanation for the repressive function of Bcl3. The fact that Bcl3 does not affect promotility genes suggests that Bcl3 de-represses cell motility in tumor cells with prometastatic oncogenic lesions. This is supported by recent unpublished data from our laboratory showing that the migratory capacity of nontumorigenic cells is not affected by Bcl3 suppression (Soukupova, unpublished). A recent study by Merkhofer and colleagues showed that downregulation of canonical NF-κB activity in an ERBB2-positive human breast cancer cell line resulted in a decrease in invasive properties *in vitro* but had no effect on cell proliferation (26). ERBB2-driven cell proliferation in these cells was attributed to phosphoinositide 3-kinase (PI3K) signaling independently of NF-κB, suggesting that these 2two signaling pathways have different roles downstream of ERBB2. It is possible therefore that in the current study of ERBB2-positive tumors, Bcl3 is able to modify canonical NF-κB signaling to specifically exert a prometastatic rather than proproliferative effect on this tumor subtype.

Loss of Stat3 has also previously been shown to delay the metastatic progression of ERBB2-positive tumors both via direct cell-autonomous mechanisms and through inflammatory mediators (4). Stat3, like NF-κB, is upregulated in many malignancies including breast cancer (52) but is paradoxically proapoptotic during mammary involution (18). As *Bcl3* is a downstream transcriptional target of Stat3, we suggest that Bcl3 acts as a molecular link between Stat3 and NF-κB and consequently may contribute to the metastatic phenotypes mediated by these transcription pathways. Furthermore, like NF-κB, as constitutive inhibition of Stat3 is detrimental to normal tissue homeostasis and cellular immunity in the adult (53, 54), it will be interesting in the future to determine the effect of conditionally suppressing Bcl3 in breast cancer models where Stat3 and/or NF-κB activities are aberrantly activated to determine its therapeutic efficacy.

In addition to the profound reduction in metastatic tumor burden, we also observed a significant decrease in the ratio of proliferating versus apoptotic cells in the secondary lesions, an effect not seen at the primary site. We postulate that the microenvironment of the respective tumors may play a role in this, possibly through the activation of a distinct NF-κB/Bcl3 signaling pathway in the lesions within the lung, that are more focused on cell turnover. While we have yet to determine the identity of this pathway, it is clear that if mirrored in humans, this potential reduction in tumor growth at the secondary site could contribute significantly to the overall reduction in tumor burden in patients with HER2-positive breast cancer.

Current work is therefore focusing on the mechanism of secondary tumor growth in this model and whether the beneficial effects of Bcl3 suppression are recapitulated in human breast cancers.

Disclosure of Potential Conflicts of Interest

No potential conflicts of interest were disclosed.

Published OnlineFirst November 13, 2012; DOI: 10.1158/0008-5472.CAN-12-1321

Authors' Contributions

Conception and design: R.W.E. Clarkson
Development of methodology: A. Wakefield, J. Soukupova, R.W.E. Clarkson
Acquisition of data (provided animals, acquired and managed patients, provided facilities, etc.): A. Wakefield, A. Montagne, R. French, W. Muller, R.W.E. Clarkson
Analysis and interpretation of data (e.g., statistical analysis, biostatistics, computational analysis): A. Wakefield, J. Soukupova, A. Montagne. J.J. Ranger, R.W.E. Clarkson
Writing, review, and/or revision of the manuscript: A. Wakefield, R.W.E. Clarkson
Study supervision: R.W.E. Clarkson

Acknowledgments

J. Soukupova is currently a Cardiff University President's PhD Scholar. The authors thank Emma Blain, Dawn Croston, Natalie Card, and Sabine Schmidt for technical assistance and Prof. Alan Clarke for critical assessment of the manuscript.

Grant Support

This study was funded by the Breast Cancer Research Trust UK, Breast Cancer Campaign and seedcorn funding from Cardiff University School of Biosciences. R.W.E. Clarkson was funded by a Research Council-UK Research Fellowship. A. Wakefield was supported by an MRC PhD studentship.

The costs of publication of this article were defrayed in part by the payment of page charges. This article must therefore be hereby marked *advertisement* in accordance with 18 U.S.C. Section 1734 solely to indicate this fact.

Received April 5, 2012; revised August 31, 2012; accepted October 22, 2012; published OnlineFirst November 13, 2012.

References

1. Slamon DJ, Leyland-Jones B, Shak S, Fuchs H, Paton V, Bajamonde A, et al. Use of chemotherapy plus a monoclonal antibody against HER2 for metastatic breast cancer that overexpresses HER2. N Engl J Med 2001;344:783–92.
2. Viani GA, Afonso SL, Stefano EJ, De Fendi LI, Soares FV. Adjuvant trastuzumab in the treatment of her-2-positive early breast cancer: a meta-analysis of published randomized trials. BMC Cancer 2007;7:153.
3. Hartman ZC, Yang XY, Glass O, Lei G, Osada T, Dave SS, et al. HER2 overexpression elicits a proinflammatory IL-6 autocrine signaling loop that is critical for tumorigenesis. Cancer Res 2011;71:4380–91.
4. Ranger JJ, Levy DE, Shahalizadeh S, Hallett M, Muller WJ. Identification of a Stat3-dependent transcription regulatory network involved in metastatic progression. Cancer Res 2009;69:6823–30.
5. Clarkson RW, Boland MP, Kritikou EA, Lee JM, Freeman TC, Tiffen PG, et al. The genes induced by signal transducer and activators of transcription (STAT)3 and STAT5 in mammary epithelial cells define the roles of these STATs in mammary development. Mol Endocrinol 2006;20:675–85.
6. Bours V, Franzoso G, Azarenko V, Park S, Kanno T, Brown K, et al. The oncoprotein Bcl-3 directly transactivates through kappa B motifs via association with DNA-binding p50B homodimers. Cell 1993;72:729–39.
7. Cogswell PC, Guttridge DC, Funkhouser WK, Baldwin AS Jr. Selective activation of NF-kappa B subunits in human breast cancer: potential roles for NF-kappa B2/p52 and for Bcl-3. Oncogene 2000;19:1123–31.
8. Massoumi R, Chmielarska K, Hennecke K, Pfeifer A, Fassler R. Cyld inhibits tumor cell proliferation by blocking Bcl-3-dependent NF-kappaB signaling. Cell 2006;125:665–77.
9. Guan Y, Yao H, Zheng Z, Qiu G, Sun K. MiR-125b targets BCL3 and suppresses ovarian cancer proliferation. Int J Cancer 2011;128:2274–83.
10. Park SG, Chung C, Kang H, Kim JY, Jung G. Up-regulation of cyclin D1 by HBx is mediated by NF-kappaB2/BCL3 complex through kappaB site of cyclin D1 promoter. J Biol Chem 2006;281:31770–7.
11. Rocha S, Martin AM, Meek DW, Perkins ND. p53 represses cyclin D1 transcription through down regulation of Bcl-3 and inducing increased association of the p52 NF-kappaB subunit with histone deacetylase 1. Mol Cell Biol 2003;23:4713–27.
12. Kashatus D, Cogswell P, Baldwin AS. Expression of the Bcl-3 proto-oncogene suppresses p53 activation. Genes Dev 2006;20:225–35.
13. Clarkson RW, Heeley JL, Chapman R, Aillet F, Hay RT, Wyllie A, et al. NF-kappaB inhibits apoptosis in murine mammary epithelia. J Biol Chem 2000;275:12737–42.
14. Helbig G, Christopherson KW II, Bhat-Nakshatri P, Kumar S, Kishimoto H, Miller KD, et al. NF-kappaB promotes breast cancer cell migration and metastasis by inducing the expression of the chemokine receptor CXCR4. J Biol Chem 2003;278:21631–8.
15. Park BK, Zhang H, Zeng Q, Dai J, Keller ET, Giordano T, et al. NF-kappaB in breast cancer cells promotes osteolytic bone metastasis by inducing osteoclastogenesis via GM-CSF. Nat Med 2007;13:62–9.
16. Aggarwal BB, Shishodia S, Takada Y, Banerjee S, Newman RA, Bueso-Ramos CE, et al. Curcumin suppresses the paclitaxel-induced nuclear factor-kappaB pathway in breast cancer cells and inhibits lung metastasis of human breast cancer in nude mice. Clin Cancer Res 2005;11:7490–8.
17. Clarkson RW, Watson CJ. NF-kappaB and apoptosis in mammary epithelial cells. J Mammary Gland Biol Neoplasia 1999;4:165–75.
18. Chapman RS, Lourenco PC, Tonner E, Flint DJ, Selbert S, Takeda K, et al. Suppression of epithelial apoptosis and delayed mammary gland involution in mice with a conditional knockout of Stat3. Genes Dev 1999;13:2604–16.
19. Guy CT, Webster MA, Schaller M, Parsons TJ, Cardiff RD, Muller WJ. Expression of the neu protooncogene in the mammary epithelium of transgenic mice induces metastatic disease. Proc Natl Acad Sci U S A 1992;89:10578–82.
20. Schwarz EM, Krimpenfort P, Berns A, Verma IM. Immunological defects in mice with a targeted disruption in Bcl-3. Genes Dev 1997;11:187–97.
21. Sacco MG, Gribaldo L, Barbieri O, Turchi G, Zucchi I, Collotta A, et al. Establishment and characterization of a new mammary adenocarcinoma cell line derived from MMTV neu transgenic mice. Breast Cancer Res Treat 1998;47:171–80.
22. Tiffen PG, Omidvar N, Marquez-Almuina N, Croston D, Watson CJ, Clarkson RW. A dual role for oncostatin M signaling in the differentiation and death of mammary epithelial cells *in vivo*. Mol Endocrinol 2008;22:2677–88.
23. Smyth GK. Linear models and empirical bayes methods for assessing differential expression in microarray experiments. Stat Appl Genet Mol Biol 2004;3:Article3.
24. Liu M, Ju X, Willmarth NE, Casimiro MC, Ojeifo J, Sakamaki T, et al. Nuclear factor-kappaB enhances ErbB2-induced mammary tumorigenesis and neoangiogenesis *in vivo*. Am J Pathol 2009;174:1910–20.
25. Cao Y, Luo JL, Karin M. IkappaB kinase alpha kinase activity is required for self-renewal of ErbB2/Her2-transformed mammary tumor-initiating cells. Proc Natl Acad Sci U S A 2007;104:15852–7.
26. Merkhofer EC, Cogswell P, Baldwin AS. Her2 activates NF-kappaB and induces invasion through the canonical pathway involving IKKalpha. Oncogene 2010;29:1238–48.
27. Bundred NJ, Anderson E, Nicholson RI, Dowsett M, Dixon M, Robertson JF. Fulvestrant, an estrogen receptor downregulator, reduces cell turnover index more effectively than tamoxifen. Anticancer Res 2002;22:2317–9.
28. Baxter FO, Came PJ, Abell K, Kedjouar B, Huth M, Rajewsky K, et al. IKKbeta/2 induces TWEAK and apoptosis in mammary epithelial cells. Development 2006;133:3485–94.
29. Brantley DM, Chen CL, Muraoka RS, Bushdid PB, Bradberry JL, Kittrell F, et al. Nuclear factor-kappaB (NF-kappaB) regulates proliferation and branching in mouse mammary epithelium. Mol Biol Cell 2001;12:1445–55.
30. Cao Y, Bonizzi G, Seagroves TN, Greten FR, Johnson R, Schmidt EV, et al. IKKalpha provides an essential link between RANK signaling and cyclin D1 expression during mammary gland development. Cell 2001;107:763–75.
31. Pratt MA, Tibbo E, Robertson SJ, Jansson D, Hurst K, Perez-Iratxeta C, et al. The canonical NF-kappaB pathway is required for formation of

Published OnlineFirst November 13, 2012; DOI: 10.1158/0008-5472.CAN-12-1321

luminal mammary neoplasias and is activated in the mammary progenitor population. Oncogene 2009;28:2710–22.
32. Grange C, Lanzardo S, Cavallo F, Camussi G, Bussolati B. Sca-1 identifies the tumor-initiating cells in mammary tumors of BALB-neuT transgenic mice. Neoplasia 2008;10:1433–43.
33. Huang S, Chen Y, Podsypanina K, Li Y. Comparison of expression profiles of metastatic versus primary mammary tumors in MMTV-Wnt-1 and MMTV-Neu transgenic mice. Neoplasia 2008;10: 118–24.
34. Horak CE, Lee JH, Elkahloun AG, Boissan M, Dumont S, Maga TK, et al. Nm23-H1 suppresses tumor cell motility by down-regulating the lysophosphatidic acid receptor EDG2. Cancer Res 2007;67:7238–46.
35. McDermott WG, Boissan M, Lacombe ML, Steeg PS, Horak CE. Nm23-H1 homologs suppress tumor cell motility and anchorage independent growth. Clin Exp Metastasis 2008;25:131–8.
36. Boissan M, Wendum D, Arnaud-Dabernat S, Munier A, Debray M, Lascu I, et al. Increased lung metastasis in transgenic NM23-Null/SV40 mice with hepatocellular carcinoma. J Natl Cancer Inst 2005;97: 836–45.
37. Moissoglu K, McRoberts KS, Meier JA, Theodorescu D, Schwartz MA. Rho GDP dissociation inhibitor 2 suppresses metastasis via unconventional regulation of RhoGTPases. Cancer Res 2009;69: 2838–44.
38. Garcia-Mata R, Boulter E, Burridge K. The 'invisible hand': regulation of RHO GTPases by RHOGDIs. Nat Rev Mol Cell Biol 2011;12: 493–504.
39. Hu LD, Zou HF, Zhan SX, Cao KM. Biphasic expression of RhoGDI2 in the progression of breast cancer and its negative relation with lymph node metastasis. Oncol Rep 2007;17:1383–9.
40. Bourboulia D, Stetler-Stevenson WG. Matrix metalloproteinases (MMPs) and tissue inhibitors of metalloproteinases (TIMPs): Positive and negative regulators in tumor cell adhesion. Semin Cancer Biol 2010;20:161–8.
41. Thornburg NJ, Pathmanathan R, Raab-Traub N. Activation of nuclear factor-kappaB p50 homodimer/Bcl-3 complexes in nasopharyngeal carcinoma. Cancer Res 2003;63:8293–301.
42. Pallares J, Martínez-Guitarte JL, Dolcet X, Llobet D, Rue M, Palacios J, et al. Abnormalities in the NF-kappaB family and related proteins in endometrial carcinoma. J Pathol 2004;204:569–77.
43. Puvvada SD, Funkhouser WK, Greene K, Deal A, Chu H, Baldwin AS, et al. NF-kB and Bcl-3 activation are prognostic in metastatic colorectal cancer. Oncology 2010;78:181–8.
44. Pratt MA, Bishop TE, White D, Yasvinski G, Ménard M, Niu MY, et al. Estrogen withdrawal-induced NF-kappaB activity and bcl-3 expression in breast cancer cells: roles in growth and hormone independence. Mol Cell Biol 2003;23:6887–900.
45. Karin M. Nuclear factor-kappaB in cancer development and progression. Nature 2006;441:431–6.
46. Kim HJ, Hawke N, Baldwin AS. NF-kappaB and IKK as therapeutic targets in cancer. Cell Death Differ 2006;13:738–47.
47. Palmer S, Chen YH. Bcl-3, a multifaceted modulator of NF-kappaB-mediated gene transcription. Immunol Res 2008;42:210–8.
48. Franzoso G, Bours V, Azarenko V, Park S, Tomita-Yamaguchi M, Kanno T, et al. The oncoprotein Bcl-3 can facilitate NF-kappa B-mediated transactivation by removing inhibiting p50 homodimers from select kappa B sites. EMBO J 1993;12:3893–901.
49. Maldonado V, Espinosa M, Pruefer F, Patiño N, Ceballos-Canciono G, Urzua U, et al. Gene regulation by BCL3 in a cervical cancer cell line. Folia Biol (Praha) 2010;56:183–93.
50. Maldonado V, Melendez-Zajgla J. Role of Bcl-3 in solid tumors. Mol Cancer 2011;10:152.
51. Choi HJ, Lee JM, Kim H, Nam HJ, Shin HJ, Kim D, et al. Bcl3-dependent stabilization of CtBP1 is crucial for the inhibition of apoptosis and tumor progression in breast cancer. Biochem Biophys Res Commun 2010;400:396–402.
52. Hsieh FC, Cheng G, Lin J. Evaluation of potential Stat3-regulated genes in human breast cancer. Biochem Biophys Res Commun 2005; 335:292–9.
53. Mankan AK, Greten FR. Inhibiting signal transducer and activator of transcription 3: rationality and rationale design of inhibitors. Expert Opin Investig Drugs 2011;20:1263–75.
54. Takeda K, Noguchi K, Shi W, Tanaka T, Matsumoto M, Yoshida N, et al. Targeted disruption of the mouse Stat3 gene leads to early embryonic lethality. Proc Natl Acad Sci U S A 1997;94:3801–4.
55. Clarkson RW, Wayland MT, Lee J, Freeman T, Watson CJ. Gene expression profiling of mammary gland development reveals putative roles for death receptors and immune mediators in post-lactational regression. Breast Cancer Res 2004;6:R92–109.

Published OnlineFirst November 13, 2012; DOI: 10.1158/0008-5472.CAN-12-1321

Cancer Research
The Journal of Cancer Research (1916–1930) | The American Journal of Cancer (1931–1940)

AACR American Association for Cancer Research

Bcl3 Selectively Promotes Metastasis of ERBB2-Driven Mammary Tumors

Alison Wakefield, Jitka Soukupova, Amelie Montagne, et al.

Cancer Res 2013;73:745-755. Published OnlineFirst November 13, 2012.